JOURNAL OF SOLID STATE CHEMISTRY 37, 24–36 (1981)

Phase Relations in the Sn–W–O Ternary System Near to WO_3

THOMMY EKSTRÖM,* M. PARMENTIER,[1] AND R. J. D. TILLEY†

**Department of Inorganic Chemistry, Arrhenius Laboratory, University of Stockholm, S-10691 Stockholm, Sweden, and †School of Materials Science, University of Bradford, Bradford BD7 1DP, W. Yorkshire, U.K.*

Received January 17, 1980; in final form April 24, 1980

Phase relations in the Sn–W–O system for compositions near to WO_3 and temperatures up to 1173 K have been determined by electron microscopy and X-ray diffraction. The phase limits for the bronzes previously reported in this system have been determined. For the orthorhombic I bronzes the phase limits are from $Sn_{0.04}WO_3$ to $Sn_{0.06}WO_3$. Two orthorhombic II bronze phases form, one at a composition of $Sn_{0.13}WO_3$ to $Sn_{0.15}WO_3$, and another at $Sn_{0.16}WO_3$. These bronzes have structures which consist of lamellae of WO_3 united by fault planes. The other bronze phase to form, with the tetragonal tungsten bronze structure, has a lower composition limit of $Sn_{0.21}WO_3$.

Introduction

Since the report of a tin tungsten bronze of the tetragonal tungsten bronze (*T T B*) type by Gier *et al.* (*1*) a number of publications have appeared concerning the chemistry of these materials (*2–5*), which includes an overall phase analysis of the Sn–W–O system (*6*) based upon single crystal X-ray diffraction studies. However, the phases found in the region close to WO_3 are complex. Many of the phases are disordered and possess large unit cells with closely related structures, making exact X-ray analysis difficult. For this reason the phase region close to WO_3 has been reinvestigated using electron microscopy as well as other techniques, to clarify some aspects of the phase relations in this system.

The results, which are in broad agreement with those published earlier, are used as a basis for a comparison of the phases found when WO_3 is reacted with the other commonly occurring Group *IV*A and *IV*B ions, viz. Ti (*7*), Zr (*8, 9*), Ge (*10, 11*), and Pb (*12*) which have been studied by us previously.

Experimental

All preparations were made by heating together tin metal and WO_3 powder in evacuated sealed silica ampoules. Appropriate amounts of these materials were thoroughly mixed and the ampoules used were as full as conveniently possible. These were put into borings in a heavy steel cylinder in the furnace because the high volatility of the tin oxide species made it desirable to minimize any temperature gradient within the ampoules.

The WO_3 was either of Specpure grade (from Johnson and Matthey Ltd.) or prepared by heating tungstic acid (from Matheson, Coleman and Bell, p.a.) in air for

[1] On leave from Laboratoire de Chimie Minerale A, University de Nancy, 54037 Nancy Cedex, France.

0022-4596/81/040024-13$02.00/0

several days at 1073 K. The tin metal was of Specpure grade (Johnson and Matthey Ltd.) or of Analytical grade (Baker's Analyzed).

The samples were heated at 973, 1073, and 1173 K for periods of time usually varying from 1 to 3 weeks. One series of samples was also heated at 1173 K for 2 months and another series at 873 K for 1 month, divided into two periods of 2 weeks, with careful grinding between heat treatments in order to homogenize the samples. All samples were quickly removed from the furnace after heating and tipped out of the steel cylinder onto an asbestos plate, but no particular precautions were taken to quench them specially rapidly. The compositions prepared are shown in Fig. 1.

The products of reaction were examined optically using a Zeiss Ultraphot optical microscope and by transmission electron microscopy using a JEM 100B electron microscope fitted with a goniometer stage and operated at 100 kV. Electron microscope specimens were prepared by crushing crystals in an agate mortar under *n*-butanol and allowing a drop of the resultant suspension to dry on a net-like carbon film. Only those crystal fragments which projected over holes in the film were examined in detail. Selected samples were also studied with a JSM 35 scanning electron microscope.

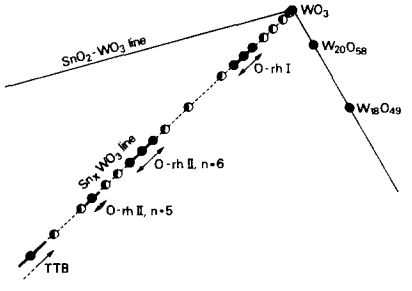

FIG. 1. Part of the phase diagram of the Sn–W–O system near to WO_3 at 1173 K. The circles represent compositions prepared in this study. Filled circles represent samples which were monophasic and half filled circles represent samples which were biphasic to X-ray powder diffraction.

All samples were investigated by recording their X-ray powder patterns at room temperature in a Guinier–Hägg focusing camera using $CuK\alpha_1$ radiation (λ = 0.154051 nm) and KCl (a = 0.62919 nm) as an internal standard. The positions of the lines on the film were determined either visually or by means of an automatic Abrahamsson film scanner (*13*). Evaluation of the film data and indexing and refinement of the unit cell parameters by least-squares techniques were performed on an IBM 1800 computer, using programs written by Brandt and Nord (*14*).

Results

All the results obtained from the varying techniques employed were in good agreement with one another and allowed the partial phase diagram shown in Fig. 1 to be constructed. They are also in agreement with the previous data on this system where overlap occurs (*1–6*). The different phase regions found are described in more detail in the sections which follow.

Orthorhombic I Bronzes

These phases, originally reported by Steadman *et al.* (*3*), form for lowest tin concentrations. Optical and scanning electron microscopy are useful in the lower part of the phase range at compositions close to WO_3, as the orthorhombic bronzes form large flat platelike crystals, while the WO_3 is of a rather chunky habit. This is illustrated in Fig. 2a. Thus samples Sn_xWO_3 where x = 0.005, 0.01, 0.02, and 0.03 could readily be seen to be biphasic, a feature also found by powder X-ray diffraction. The X-ray results showed that WO_3 persisted into compositions of overall stoichiometry $Sn_{0.03}WO_3$ regardless of heating time. In $Sn_{0.04}WO_3$ samples heated for a long time WO_3 was not present, although

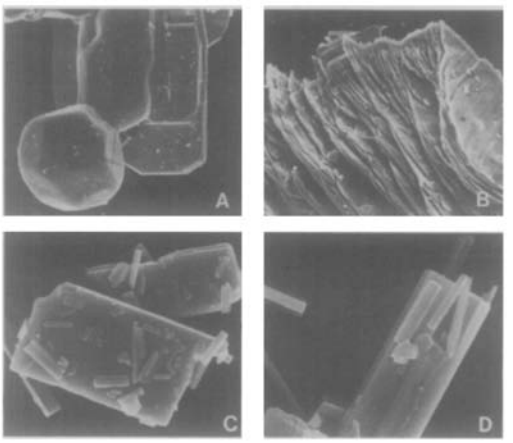

FIG. 2. Scanning electron micrographs of typical Sn_xWO_3 bronze crystals. (a) Crystals from a sample of overall composition $Sn_{0.01}$ WO_3 showing the different habits of the orthorhombic I crystals (platelike) and WO_3 (dodecahedron like). (b) The fracture edge of an orthorhombic I crystal from the same sample as (a) showing the lamellar structure of the plate. (c) Crystals from a sample of overall composition $Sn_{0.12}WO_3$ showing plate-like crystals of the $n = 5$ orthorhombic II bronze phase. (d) Crystals from the same sample as (c) showing that the orthorhombic II crystals fracture to rods rather than plates. Magnifications are (a) ×50, (b) ×90, (c) ×200, and (d) ×4000.

traces were seen in shorter heated samples. This, and the electron microscope results indicate that the lower phase limit of the orthorhombic I phases is close to $Sn_{0.04}WO_3$ at temperatures of 973–1173 K.

X-Ray results show that the orthorhombic phases exist alone in samples of overall composition from $Sn_{0.04}WO_3$ to $Sn_{0.06}WO_3$. However, equilibrium is hard to achieve in this system, and it is possible that this rather narrow range may change somewhat under different preparation conditions or at different temperatures. The findings by optical and scanning electron microscopy within this interval showed that only the plate-like crystals or fragments of these were present. A characteristic feature of these crystal plates was that they were built of thin crystal blades stacked upon top of each other like a deck of cards. Figure 2b shows a scanning electron micrograph of a fractured edge of such a plate, clearly showing the stacking disorder typically found to be present.

In samples richer in Sn, viz $x \geq 0.07$, crystals of another size or habit were found to be present. These were considerably smaller and formed as thin rods, rod-like plates or plates, which were physically separated from the large plates of the orthorhombic I bronze. Powder X-ray diffraction showed the presence of another phase or phases in these samples. In the $Sn_{0.12}WO_3$ preparation only traces of the orthorhombic I phases could be seen and this composition represents, therefore, approximately the highest x-value in which these phases can coexist together with other oxides, under the preparation conditions used in this study.

Transmission electron microscopy confirmed the presence of orthorhombic I bronzes in samples of overall composition between and including $Sn_{0.005}WO_3$ to $Sn_{0.12}WO_3$. The electron diffraction patterns of these materials are characteristic and easily recognized. They consist of an almost square array of intense subcell spots from the WO_3 matrix and rows of superlattice spots along one of these directions which we will designate as a here. The superlattice reflections have a variable periodicity and reach a maximum in intensity at the subcell position, approximately every nth, $2n$th, $3n$th etc. reflection. It is therefore convenient to refer to these phases by the value of n found on the diffraction patterns.

Typical examples illustrating this are shown in Fig. 3. In general the value of n increases as the tin content gets lower. The largest n value found was 16 and the lowest was 6. Samples were never totally homogeneous in the phases present, and a number of n values were found in each sample, irrespective of sample heating time. In samples with lowest tin content, close to WO_3,

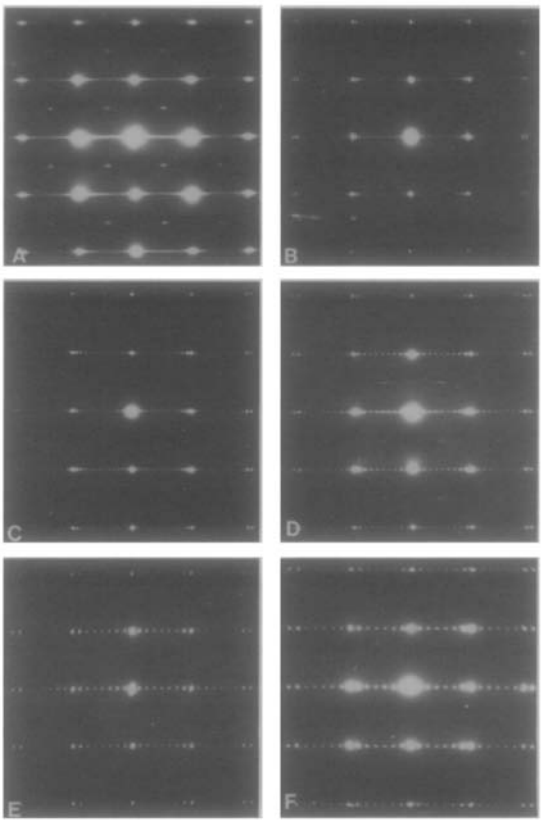

FIG. 3. Transmission electron diffraction patterns from Sn_xWO_3 orthorhombic I bronzes: (a) streaked, from a severely disordered crystal; (b) $n = 16$; (c) $n = 13$; (d) $n = 10$; (e) $n = 8$; and (f) $n = 7$. The more intense spots in a square array are due to the WO_3-like subcell and the superlattice spots lie along a^*.

the diffraction patterns were often streaked along a, making the assessment of an n value impossible.

The X-ray powder patterns of the orthorhombic I bronzes reflected the disordered structures present in the samples by being rather complex. A typical example is given in Table I. It was found that many diffraction lines were unusually broad and one explanation for this is the overlap of reflections from several similar structures with somewhat different a-axes, i.e., different n-values. At higher diffraction angles some of these broad reflections could be seen to be resolved into several partly overlapping component peaks. The reflections with indices $\{0, 2k, l\}$ are, however, strong and well-defined, which might be expected as they refer to a WO_3 subcell. These latter reflections also seemed not to broaden significantly at high diffraction angles, which indicates that the two shorter axes b and c of the series of orthorhombic I bronzes must be very similar, taking values $b \simeq 0.734$ nm and $c \simeq 0.390$ nm. This observation is in agreement with previous findings (*3*) and arises from the very similar structural building of the phases along these two crystallographic directions.

High-resolution electron microscopy of these phases showed that the structures consisted of slabs of a WO_3-like structure separated by fault planes. This is in good agreement with the structures previously reported for these materials. At lowest tin compositions the fault planes were disordered, as shown in Fig. 4. It is noteworthy that although somewhat greater disorder than that shown in Fig. 4 was sometimes met with, crystals which could be regarded as consisting of WO_3 with only one or two isolated faults were never found. In most fragments of orthorhombic I bronze crystals examined the fault planes were fairly well ordered. As is usual in these sorts of phases, mistakes do occur in the regular spacing of the fault planes but ordering seems to be the general rule. Figure 5 shows an example of a typical crystal fragment of this sort. The resolution does not allow a clarification of the structure within the fault planes, and at the moment this structure, and the position and environment of the tin ions in these phases is still uncertain.

On rare occasions, diffraction patterns superficially similar to those in Fig. 3, but differing in the arrangement of the intensities of the superlattice spots, were observed, as shown in Fig. 6. Examination of

TABLE I

THE X-RAY POWDER PATTERN OF A SAMPLE OF OVERALL COMPOSITION $Sn_{0.05}WO_3$[a,b]

Observed values					7-type		8-type		9-type	
d(nm)	I	$\|F\|^2$	Note	$\sin^2\theta \times 10^5$	$\sin^2\theta_{calc} \times 10^5$	hkl	$\sin^2\theta_{calc} \times 10^5$	hkl	$\sin^2\theta_{calc} \times 10^5$	hkl
0.5051	12	5		2325	2325	500				
0.3900	1558	1266		3900	3893	001	3893	001	3893	001
0.3797	6	5		4115					4123	201
0.3759	7	6		4199			4173	201		
0.3666	1260	1169		4415	4408	020	4408	020	4408	020
~0.3611	~420	~400	Very broad	~4550	4501 4557	120 700	4523 4532	301 710	4465	120
~0.3565	~540	~520	Very broad	~4667	4730	301	4688	220	4638 4658	220 900
0.3373	7	7		5216	5245	320			5225	211
0.3104	621	825		6156			6158	520		
0.3019	16	22	Broad	6509	6483	411			6478	620
0.2924	9	13		6941			6928	620	6957	1100
0.2775	11	18		7705	7756	620				
0.2673	622	1141		8305	8301	021	8301	021	8301	021
~0.2633	~646	~1243	Very broad	~8557	8450	701	8581	221	8530	221
0.2558	409	824	Broad	9065	8965	720			9065	920
0.2384	4	9		10442	10402	1010			10435	330
0.2263	7	18		11590			11668	530		
0.2141	313	923	Broad	12944	12858	721	12932	1310	12938	1500
0.1991	173	594		14965			14931	431		
0.1952	285	1019		15567	15572	002	15572	002	15572	002
0.1893	11	41		16552					16581	1221
0.1834	396	1607		17632	17632	040	17632	040	17632	040
0.1824	584	2398	Broad	17837	17897	502	17794	412	17862	240
0.1723	228	1046		19985	19980	022	19980	022	19980	022
0.1716	72	332		20138	20129	702	20152	640		
0.1712	237	1101	Broad	20245			20260	222	20210	222
0.1660	264	1792		21532	21525	041	21525	041	21525	041

[a] Analysis by electron microscopy shows that only orthorhombic I bronzes are present, but the sample is inhomogeneous with respect to the n-values found. Most frequently crystals with n-values of the order 7 and 8 were observed. The observed $\sin^2\theta$-values are compared with calculated values, obtained by using the long lattice distances a found by Steadman *et al.* (*3*).

[b] Data were recorded at room temperature using a Guinier–Hägg camera with strictly monochromatic Cu$K\alpha_1$ radiation. The observed integrated intensities I were obtained by a film scanner process and the corresponding $|F|^2$ values after correction for polarization, Lorentz and geometric factors were obtained by computer routines (*13, 14*). The $\sin^2\theta_{calc}$-values for the 7-, 8-, and 9-type have been calculated by using the a-axes of 2.53, 2.91, and 3.21 nm, respectively. The b- and c-axis have been the same 0.7337 and 0.3904 nm, respectively. No attempts have been made to refine the cell parameters.

these patterns shows that the superlattice spot array consists of two subsets of spots, one of which falls in intensity as the other set increases, and vice versa. Electron micrographs showed that this effect is due to an ordered intergrowth of two different orthorhombic I bronzes with n values differing by one. Thus the diffraction pattern shown in Fig. 6a is due to the ordered array $n_1 = 6$ and $n_2 = 7$, as is revealed in the

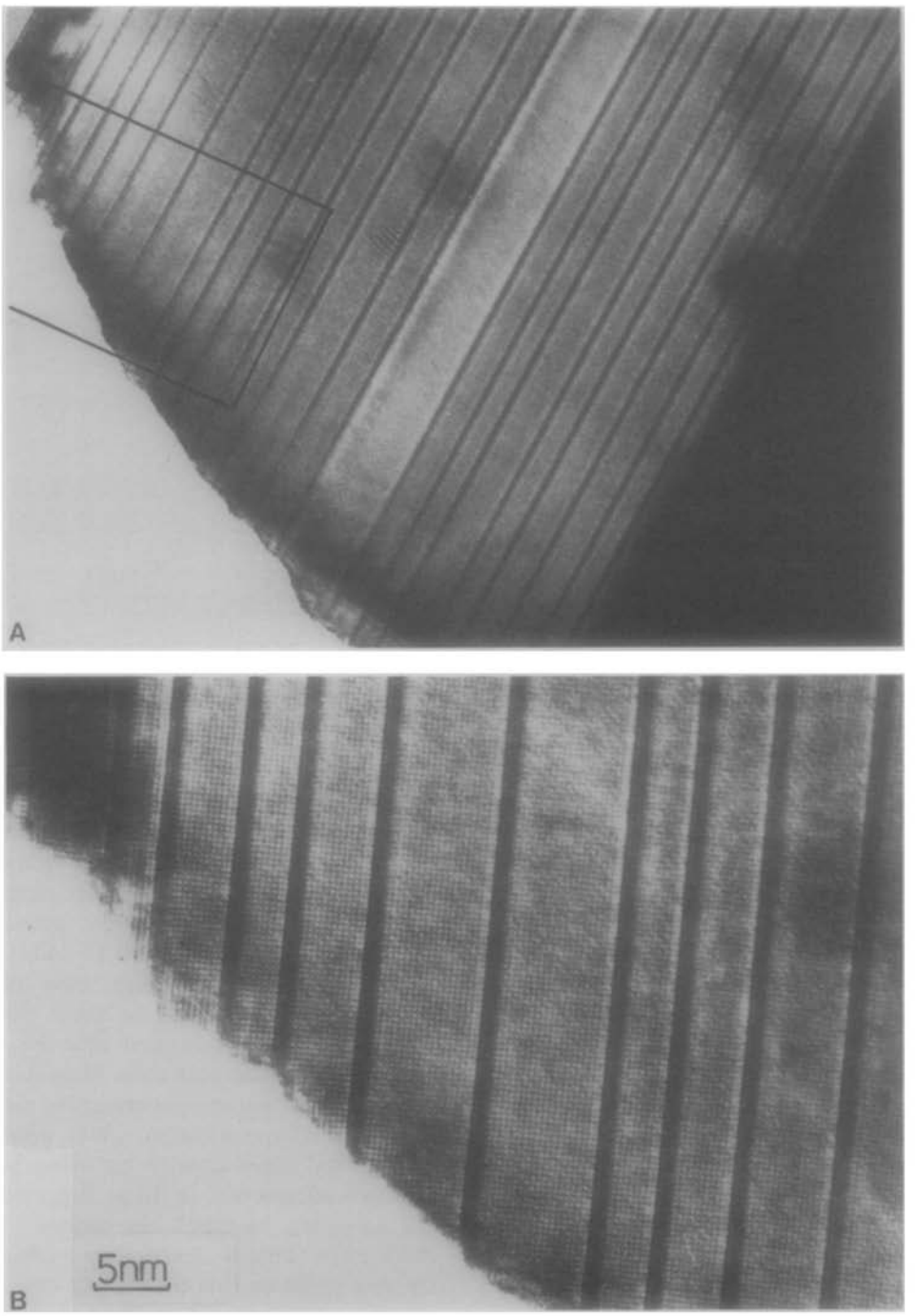

FIG. 4. (a) Low magnification electron micrograph of a disordered orthorhombic I bronze crystal fragment taken from a sample of overall composition $Sn_{0.01}WO_3$. (b) A high magnification image of the part of (a) outlined, showing that the structure of the crystal consists of lamellae of WO_3 (dotted contrast) united by fault planes which are imaged as dark strips.

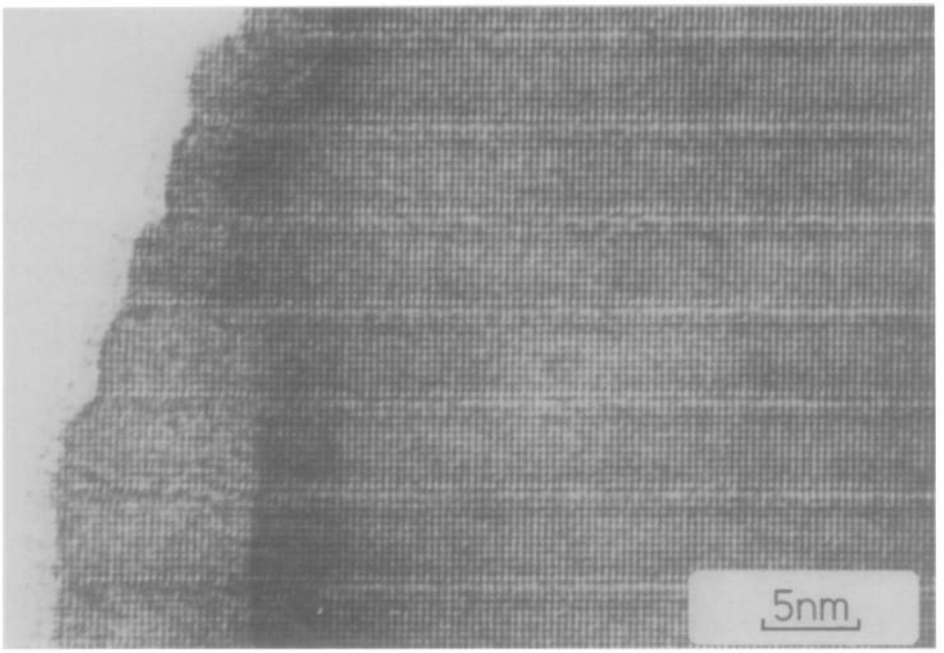

FIG. 5. Electron micrograph of a fragment of an orthorhombic I type bronze taken from a sample of overall composition $Sn_{0.02}WO_3$. Note that the edge has fractured in steps along the fault planes which separate the WO_3-like regions of the crystal, which in this crystal can be seen to be 12 WO_6 octahedra wide.

micrograph shown as Fig. 6b. When found these areas of ordering were generally extensive. Thus Fig. 6c shows the diffraction pattern from the crystal fragment shown in Fig. 6d. This latter micrograph is taken at low magnification and shows a perfectly ordered sequence of $n_1 = 9$ and $n_2 = 10$ bronze lamellae existing over the whole of the crystal flake examined.

The experiments at 873 K were principally conducted to determine whether a perovskite related bronze phase forms at lower temperatures. No such phase was found and the orthorhombic I bronzes occur, as at higher temperatures.

Orthorhombic II Phases

In samples of overall composition $Sn_{0.13}WO_3$ to $Sn_{0.15}WO_3$ X-ray diffraction suggested that only one phase was present in the samples. Increasing tin content clearly showed the presence of another phase in the samples $Sn_{0.16}WO_3$ and higher tin contents. This latter phase seemed to have a very narrow homogeneity range at $x = 0.18$ as other oxides were present in preparations in which $x = 0.17$ and 0.19.

We have termed these two phases orthorhombic II phases as their electron diffraction patterns suggest that they possess orthorhombic unit cells. However, the X-ray powder pattern recorded for samples of overall composition $Sn_{0.15}WO_3$ could not be indexed satisfactorily by using similar unit cell parameters to those suggested for the so-called "6-type" tin bronze (*3*), as detailed in Table II. A tentative explanation for this might be that the sample contains a significant amount of another very similar structure besides the "6-type" or that this phenomena might reflect an ordered intergrowth between 6- and 5-types at a unit cell

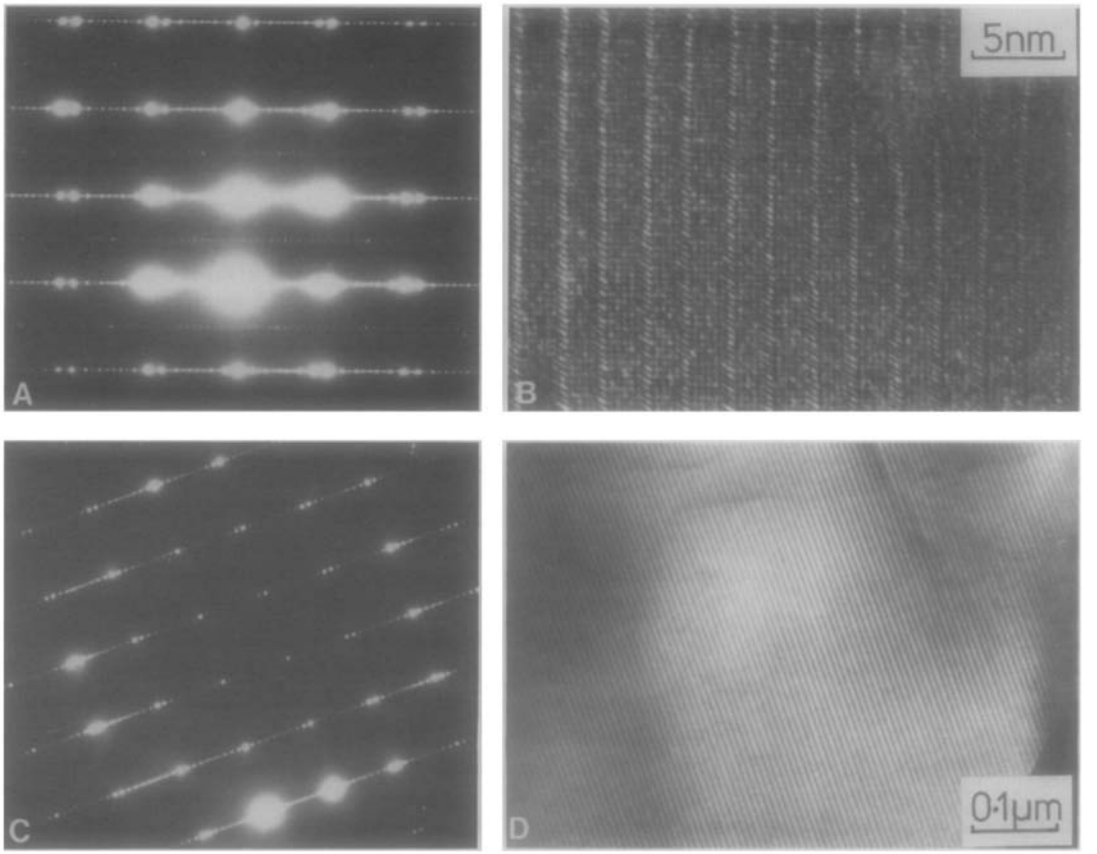

FIG. 6. (a), (c) Diffraction pattern typical of the ordered n, $n + 1$ bronze structures sometimes found. Note the regular sequence of intensity changes in the superlattice spots. (b) Micrograph of the crystal fragment giving rise to the diffraction pattern in (a). Although the resolution is poor, it is shown to be a regular intergrowth of $n = 6$ and 7, bronze structures. (d) Low magnification electron micrograph of the crystal fragment giving rise to the diffraction pattern in (c), and showing ordering of $n_1 = 9$ and $n_2 = 10$ lamellae over a considerable volume of crystal.

level. The X-ray powder pattern of a phase found at $Sn_{0.18}WO_3$ was, on the other hand, easily indexed with the cell parameters proposed earlier for the "5-type" tin bronze (*3*), as listed in Table III.

The crystals of the orthorhombic II phases were much smaller than those formed by the orthorhombic I phases. This ruled out the use of optical microscopy to study details. In the scanning electron microscope samples of the former oxides looked inhomogeneous at first sight. Besides plates, again showing a stacking disorder, other crystal forms ranging from rod-like plates to rods could be seen. A more careful study showed, however, that the plates seemed to be extremely brittle and easily fractured. In this case the fragments were seldom, as expected, the plate-like blades that build the plates. Instead they were rod-like, sometimes forming rather long and thin sticks, as shown in Fig. 2.

Electron microscopy showed that the orthorhombic II phases had somewhat similar diffraction patterns to the orthorhombic I phases described above, with n values equal to 6 and 5, with, once again, the higher n values associated with the lower

TABLE II

THE X-RAY POWDER PATTERN OBTAINED FROM A SAMPLE OF OVERALL COMPOSITION $Sn_{0.15}WO_3$[a,b]

I_{obs} (nm)	I_{obs}	$\lvert F\rvert^2_{obs}$	$\sin^2\theta_{obs} \times 10^5$	$\sin^2\theta_{calc} \times 10^5$	*hkl*
0.6867	133	32	1258	1255	110
0.5940	141	46	1682	1682	210
0.5094	81	37	2287	2282	400
0.4177	15	10	3400	3394	410
0.4077	59	43	3569	3565	500
0.3785	1754	1519	4140	4140	001
0.3713	626	565	4304		
0.3652	327	306	4449	4448	020
0.3593	73	70	4596	4591	120
0.3561	44	43	4678	4677	510
0.3488	106	109	4876		
0.3436	98	104	5024	5018	220
0.3398	870	951	5140	5134	600
0.3305	49	56	5432	5423	301
0.3258	709	848	5591		
0.3214	4	4	5742	5731	320
0.3084	79	106	6237	6246	610
0.3038	47	65	5429	6422	401
0.3001	343	490	6588		
0.2966	77	112	6742	6730	420
0.2946	28	41	6836		
0.2917	75	113	6970	6987	700
0.2773	51	86	7717	7705	501
0.2746	148	256	7870		
0.2718	62	109	8029	8013	520
0.2650	436	815	8447		
0.2628	241	458	8591	8588	021

[a] The observed $\sin^2\theta$-values are compared with calculated data using a unit cell of dimensions very close to those found by Steadman *et al.* for the "6-type" of orthorhombic II bronzes (*3*).

[b] The pattern and the observed values have been obtained as described in Table I. The calculated $\sin^2\theta$-values for the orthorhombic cell have been obtained using the lattice parameters a = 2.040 nm, b = 0.7304 nm, and c = 0.3786 nm. No attempts have been made to refine these parameters further, as the pattern apparently contains some unindexable reflections by using this unit cell.

tin content of the sample. However, the electron diffraction patterns of these phases did not show such a marked periodicity in the superlattice reflections, and they are readily distinguished from the n = 5 and 6 orthorhombic I phases described above.

These phases have, from our observations, been taken as the 5-type and 6-type structures reported by Steadman *et al.* (*3, 4, 6*). However, electron microscope images, as seen in Fig. 7, were not in good agreement with the structures proposed earlier (*3, 4*) or with similar intergrowth tungsten bronze phases reported by Hussain and Kihlborg (*15*) and this question must be left open until computed electron micrographs and further X-ray studies on our actual samples have been completed. Disordered crystal flakes were also found in these materials, and this may account for the apparent stoichiometry range of the phase occurring at the low tin composition.

TABLE III

THE X-RAY POWDER PATTERN OF AN APPARENTLY MONOPHASIC ORTHORHOMBIC II BRONZE, WITH n = 5, RECORDED FROM A SAMPLE OF GROSS COMPOSITION $Sn_{0.18}SO_3$[a]

d_{obs}(nm)	I_{obs}	$\lvert F\rvert^2_{obs}$	$\sin^2\theta_{obs} \times 10^5$	*hkl*	Δ
0.6114	212	65	1587	310	+14
0.5541	119	46	1932	410	− 3
0.4153	18	12	3439	800	+ 2
0.3980	56	43	3746	710	+ 7
0.3789	2004	1731	4133	001	− 4
0.3712	313	283	4306	020	+ 2
0.3622	204	194	4521	220	+ 2
0.3441	148	156	5011	401	+15
0.3389	832	915	5167	420	+ 4
0.3322	660	757	5377	1000	+ 7
0.3127	59	77	6066	601	− 4
0.3083	766	1032	6241	620	+ 4
0.2798	41	68	7575	801	+ 1
0.2766	113	192	7753	820	+12
0.2750	48	82	7847	711	+ 3
0.2652	322	601	8436	021	− 5
0.2526	542	1123	9298	421	− 2
0.2497	524	1113	9515	1001	+ 8
0.2474	134	209	9689	1020	+15
0.2392	560	1305	10371	621	− 3

[a] The pattern and the observed values have been obtained in the same way as described in Table I. A calculation of the orthorhombic cell parameters gave a = 3.324 nm, b = 0.7426 nm, and c = 0.3787 nm. In the table, $\Delta = 10^5 \times (\sin^2\theta_{obs} - \sin^2\theta_{calc})$.

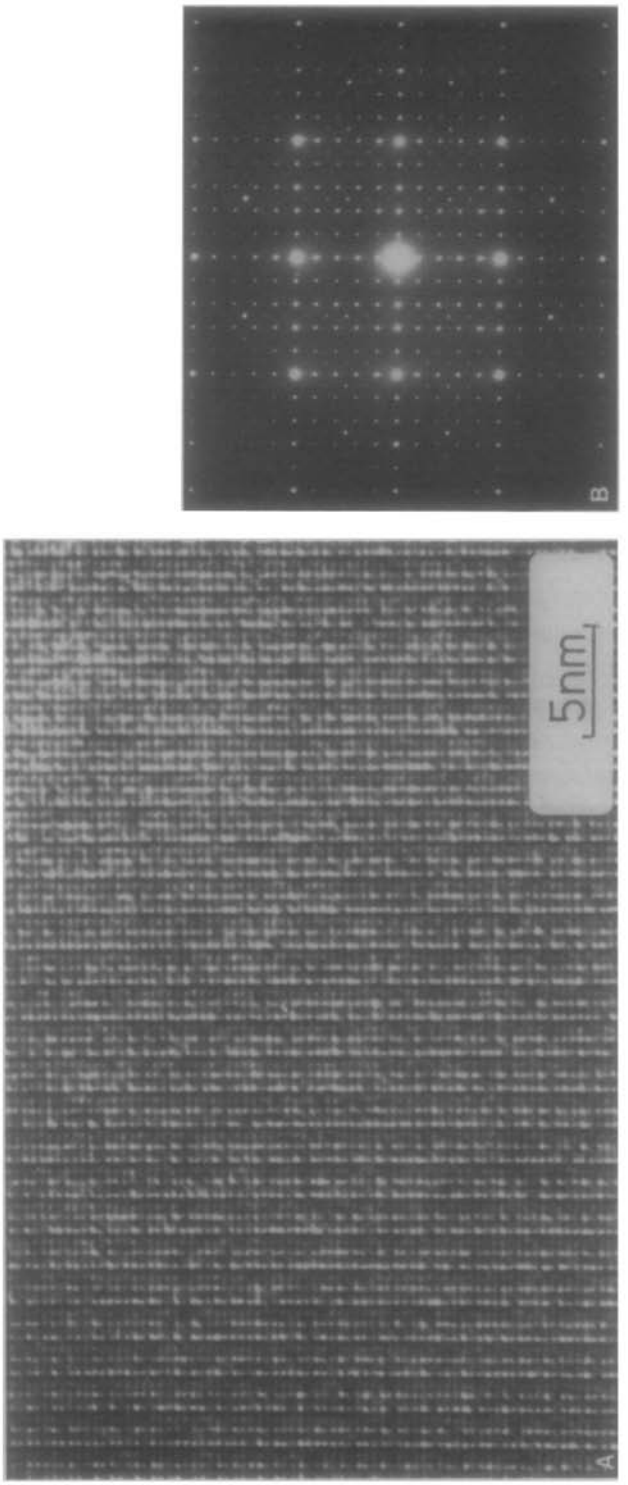

FIG. 7. (a) Electron micrograph and (b) diffraction pattern from a crystal fragment of an orthorhombic II 5 type bronze; taken from a sample of overall composition $Sn_{0.18}WO_3$.

Another possibility here is that we could have extensive intergrowth between the two orthorhombic II phases. However further electron microscopy is needed before this behavior can be verified, as no crystals which showed this behavior were observed during the present study.

The TTB Phase

This phase was not investigated in detail in this study. The lower limit of the homogeneity range was, however, close to $x = 0.21$ as samples of this composition contained only traces of the orthorhombic II bronze besides the *TTB* oxide while in samples of composition $Sn_{0.23}WO_3$ only the *TTB* phase was observed.

Discussion

For the lowest tin content samples the results show that two-phase mixtures occur in which WO_3 and the orthorhombic I bronze are present. There is no evidence at all that a perovskite bronze forms, or that the tin atoms or ions enter into the WO_3 crystal structure. The observation that the orthorhombic I bronze phase crystals are plate-like and of quite a different habit than the WO_3 crystals suggests that they form by way of a vapor-transport process rather than by way of a solid state reaction involving the diffusion of tin species into the WO_3 matrix. A mechanism which accounts for this behavior has already been discussed with reference to analogous lead phases (*12*). This suggestion is substantiated by the microstructures of the orthorhombic I phases. If they formed by a mechanism which involves the diffusion of tin atoms or ions into the WO_3 crystalline matrix one would expect to find crystal fragments with a few isolated faults, or else small clusters of faults at the lowest tin concentrations. These faults would be expected to increase in density and degree of ordering until phases found here appeared. The fact that this does not occur is thus in agreement with the notion that reaction between vapor species is relevant.

The resolution of the electron micrographs does not permit us to say whether the tin lies in the fault planes but from a crystal chemical and mechanistic viewpoint this would seem to be reasonable. Two different models for the structure of these planes have been suggested in a previous communication concerning the analogous phase in the Pb_xWO_3 system (*12*).

The lower limit of the orthorhombic I phases appears to occur when the width of the WO_3-like lamellae reaches 5 octahedra. The morphology studies indicate that the transformation between the orthorhombic I $\rightarrow$ II phases does not take place by a solid state reaction. A growth process involving vapor species again seems to be of importance. The structures of these orthorhombic II phases could be identical to the "5-type" and "6-type" structures described by Steadman (*4*). However, as our electron images do not match the expected structures well this cannot, at this stage, be certain. Further studies involving electron microscopy and single crystal X-ray diffraction should resolve this problem and it will not be discussed further here.

Comparison with Other Group IV Elements

When we consider the group IVB elements we find that the Sn–W–O system near to WO_3 is the most complex. The behavior is closest to that of Pb, which has already been discussed in some detail in a previous communication (*12*). In the lead system we have a series of orthorhombic bronzes which appear to be almost identical to the orthorhombic I phases in the tin system with apparently similar composition range and temperature stability. The lead system does not, though, form the

orthorhombic II phases but does form the *TTB* phase.

For the case of Si and Ge, different behavior is found. Si does not react at all with WO_3, but instead forms SiO_2 leaving a residue of reduced tungsten oxides (*16*). Ge on the other hand forms a limited perovskite bronze phase below about 800 K but at higher temperatures this decomposes and the products GeO_2 and reduced tungsten oxides are the same as in the case of silicon.

When we consider the group IVA metals, information is available only for Ti–W–O (*7*) and Zr–W–O (*8, 9*) although we would presume that Hf–W–O would behave in a rather similar manner to this latter system. In the Ti–W–O oxides there is no reaction between TiO_2 and WO_3 (*16*). When reduced preparations are made, there is some reaction with WO_3 to produce ternary oxides which contain both metals. In the case of Ti, it would seem that Ti^{4+} substitutes for W^{6+} in the WO_3 matrix, and a variety of *CS* phases results (*7*). Zirconium does not appear to enjoy fairly regular octahedral coordination, and seems to form stable oxide phases with, at the moment, unknown structures, by way of a reaction path which seems to involve interpolation into WO_3 and the formation of a Zr_xWO_3 bronze.

In order to try to explain this behavior we need to take into account a number of crystal chemical factors, which include the preference of the Group IV ions for octahedral coordination, their sizes, valence, and the relative stabilities of other possible phases in the ternary *M*–W–O system. All of these factors play a part in determining which structures form in the ternary system. At higher temperatures, the M^{4+} ions Ti^{4+}, Zr^{4+}, Si^{4+}, and Ge^{4+} all tend to be stable. The ions are relatively small, and so substitution into WO_3 and the possible formation of *CS* planes, would seem to be reasonable. In reality it appears that Si^{4+} and Ge^{4+} are too small, and prefer tetrahedral coordination, while Zr^{4+} does not adopt octahedral coordination under normal circumstances, and prefers the irregular coordination found typically in ZrO_2. Ti^{4+} is thus the only candidate for a *CS* forming role in this series of compounds.

Superimposed upon this general trend is the stability of other oxides in these systems. It is well known that the stability of the MO_2 oxides is considerable. All are found as stable minerals and it is this which governs the ultimate equilibrium in these systems. Thus a consistent trend is found in which the smaller M^{4+} ions form stable MO_2 oxides by an unknown pathway, but possibly directly, while the larger Ti^{4+} and Zr^{4+} ions form stable oxides by reaction with WO_3 and subsequent disproportionation. In the one case, substitution and *CS* plane formation results (Ti) while in the other, a perovskite bronze forms (Zr), a pattern clearly controlled by the liking of the ions involved for octahedral coordination.

In the case of Ge, this ion prefers the moderately stable Ge^{2+} valence at lower temperatures. In this state it is conveniently grouped with Sn and Pb. In these latter ions the M^{2+} state is preferred at high temperatures. As all of these will be lone pair ions they would be unlikely to adopt octahedral coordination and substitute into the WO_3 structure. Instead reaction to form a perovskite bronze would be expected. This indeed happens for Ge^{2+} but in the cases of Sn^{2+} and Pb^{2+} intergrowth phases form. The reasons why this should be are unknown, but metal–metal interactions between the larger tin or lead ions may also be important in stabilizing the lamellar structure of these materials.

Acknowledgments

RJDT is indebted to the Science Research Council for an equipment grant. TE is grateful to Professor

Arne Magnéli for the experimental facilities put at his disposal and also to the Swedish Natural Science Research Council for sponsoring a part of these studies.

References

1. T. E. GIER, D. C. PEASE, A. W. SLEIGHT, AND T. A. BITHER, *Inorg. Chem.* **7**, 1646 (1968).
2. I. J. MCCOLM, R. STEADMAN, AND A. HOWE, *J. Solid State Chem.* **2**, 55 (1970).
3. R. STEADMAN, R. J. D. TILLEY, AND I. J. MCCOLM, *J. Solid State Chem.* **4**, 199 (1972).
4. R. STEADMAN, *Mater. Res. Bull.* **7**, 1143 (1972).
5. R. STEADMAN, *J. Chem. Soc. Dalton* 1972 (1972).
6. I. J. MCCOLM, R., STEADMAN, AND C. DIMBYLOW, *J. Solid State Chem.* **14**, 185 (1975).
7. T. EKSTRÖM AND R. D. J. TILLEY, *Mater. Res. Bull.* **9**, 705 (1974).
8. T. EKSTRÖM AND R. J. D. TILLEY, *Mater. Res. Bull.* **9**, 999 (1974).
9. T. EKSTRÖM AND R. J. D. TILLEY, *J. Solid State Chem.* **19**, 227 (1976).
10. M. PARMENTIER AND C. GLEITZER, *J. Solid State Chem.* **17**, 255 (1976).
11. T. EKSTRÖM, E. IGUCHI, AND R. J. D. TILLEY, *Acta Chem. Scand.* **A30**, 312 (1976).
12. T. EKSTRÖM AND R. J. D. TILLEY, *J. Solid State Chem.* **24**, 209 (1978).
13. G. MALMROS AND P. E. WERNER, *Acta Chem. Scand.* **27**, 493 (1973).
14. B. G. BRANDT AND A. G. NORD, *Chem. Commun. Univ. Stockholm* No. V (1970).
15. A. HUSSAIN AND L. KIHLBORG, *Acta Crystallogr.* **A32**, 551 (1976).
16. T. EKSTRÖM AND R. J. D. TILLEY, unpublished results.